Barton, M. H., McGeehan, J. P., & Lawton, M. C. (1992). Error rate prediction for high data rate short range systems. In 2nd Virginia Tech Symposium on Wireless Personal Communications, Virginia, USA, June 1992. (pp. 14-1 - 14-12). Virginia Polytechnic Institute and State University.

Error Rate Prediction for High Data Rate Short Range Systems

M.H. Barton, J.P. McGeehan, A.R. Nix & M.C. Lawton
Centre for Communications Research
Faculty of Engineering, University of Bristol
Queens Building, University Walk
Bristol BS8 1TR, United Kingdom
Tel: +44 22 303727, Fax: +44 272 255265

Abstract: *Present mobile radio services offer primarily voice communication to customers roaming within large cell topographies. Typically these systems do not require large bandwidths and offer little or nothing in the way of data based services with the result that they operate with bit error rates as high as one in one thousand. However, in recent years there has been a trend towards more spectrally efficient, small cell, high data rate systems and a growing demand for a new type of service offering very high data rates for indoor wireless LAN applications. In this paper we present a model which predicts propagation characteristics for given small cell environments and subsequently uses the propagation data to analyse the radio link performance for a variety of system designs. In order to achieve very accurate high data rate transmission the benefits of linear modulation combined with techniques such as diversity, frequency hopping and pulse shaping are investigated.*

1. Introduction

Current local area networks are generally wire based and typically operate at data rates up to 10 Mb/s. Replacement networks should therefore be aiming to match, or preferably improve upon, this order of performance. The ability to achieve such high speed transmissions at low error rates is severely restricted by the propagation characteristics of the surrounding environment. In particular, the spread in delay times seen at the mobile receiver tends to restrict the maximum transmission rate for a given cell coverage area [1-3]. This restriction arises as a result of *intersymbol interference* which leads to the introduction of an irreducible error floor. This paper presents some of the results obtained after modelling a number of radio environments and configurations for both indoor and outdoor applications. The simulation package makes use of predicted impulse response waveforms in order to confidently represent realistic channels. Extensive measurements have been taken in order to evaluate this propagation model. Various modulation schemes were considered, ranging from QPSK to various constellation versions of 16QAM.

In order to achieve a high data rate, systems must be able to tolerate relatively large values of normalised delay spread. Multi-level modulation schemes appear particularly attractive because they offer a gain in bandwidth efficiency which, if required, enables the use of anti-multipath pulse shapes to improve the system's ISI immunity. In addition, to operate in larger delay spreads, techniques such as diversity or channel equalisation were found to be required. However, both these techniques tend to suffer when operating in severe signal fades. This makes it difficult to guarantee the very low error rates necessary for data transfer. For example, there is always a small probability that the receiver will find itself in or slowly moving through a fade. To overcome this problem we have proposed the use of linear frequency hopping which effectively *randomises* the channel statistics. This technique, when combined with suitable channel coding, avoids the problems of the fading channel and thus allows very low error rates to be maintained at all times.

2. The Propagation Model

The equation used to describe the channel was first proposed by Turin [4] and has been subsequently used by several authors [5,6]. It takes the form of a band-limited complex impulse response, $h(t)$, given by:

$$h(t) = \sum_{k=1}^{n} \alpha_k \, \delta(t - \tau_k) \exp(j\varphi_k) \qquad (1)$$

Here the transmitted pulse is mathematically described by a Dirac function and the received signal, $h(t)$, is formed from the addition of waves

from several time delayed paths, each represented by an attenuated and phase shifted Dirac waveform. The method adopted in this paper directly seeks to evaluate suitable path parameters for the amplitude α_k, arrival time τ_k, and the arrival phase φ_k, such that the propagation characteristics can be predicted. This calculation uses geometric optics and the geometric theory of diffraction.

2.1. Geometric Optics

The algorithm uses geometric optics in order that it can calculate analytically all reflected and transmitted paths up to and including seventh order reflections for both indoor and short range outdoor microcellular applications. For the outdoor microcellular scenario the model works in two dimensions and for each calculated path an additional ground reflected ray is added. This in effect makes the assumption that the roof tops are having no impact on the results and consequently the antenna must always be placed below roof top height. Without the requirement for ceiling reflection calculations the outdoor model is capable of working with more complex cell structures. Rather than considering up to seventh order reflections at each location the algorithm evaluates up to four orders of reflection beyond that of the strongest path. Thus for a line of sight (LOS) scenario the model considers only up to only fourth order reflections, whereas should the most dominant path be of third order reflection then the algorithm considers all rays up to the seventh order of reflection. For an empty environment it is possible to generate equations for the maximum number of reflected paths up to and including a given number of reflections, n. For a 3-D box environment the maximum number of reflected paths can be calculated from the following equation:

$$P = \frac{4}{3}n^3 + 2n^2 + \frac{8}{3}n + 1 \qquad (2)$$

and for a 2-D rectangular environment (includes ground reflected rays):

$$P = 4n^2 + 4n + 2 \qquad (3)$$

Thus with an empty 3-D environment there is a maximum of 129 rays up to and including 4 reflections and a limit of 575 rays if all rays up to and including seven reflections are considered. The corresponding figures for a 2-D environment are 82 and 226 respectively.

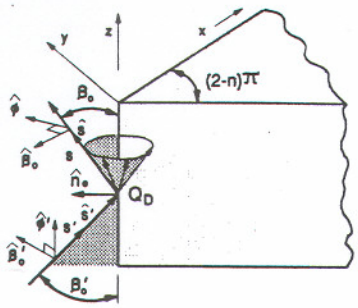

Oblique incidence

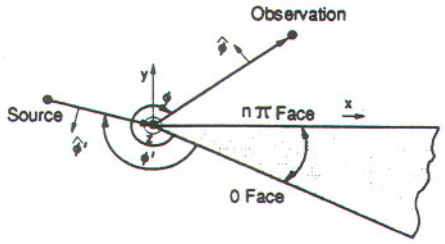

Plan view of wedge

Figure 1: Geometry of a Diffracted Path

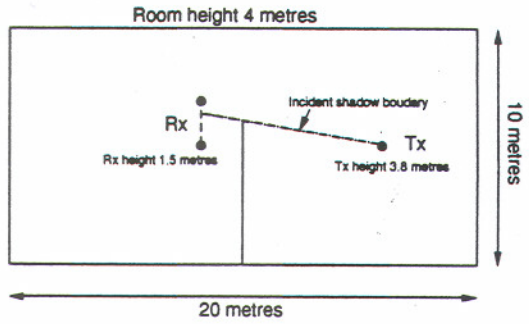

Figure 2: Diffraction Test Set-up

Conceptually the algorithm works by reflecting the transmitter about a chosen reflecting wall or walls. A line is then drawn between the receiver and transmitter image. If this is intersected by the reflecting wall and no other walls then a purely reflected path is said to exist. The value of τ_k for this path is found from the length of the line and the speed of light. α_k is found by using a square law attenuation of signal power with distance and

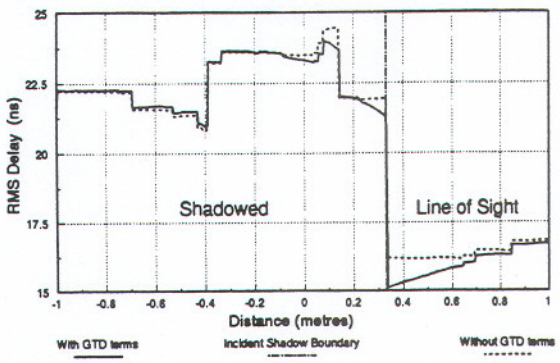

Figure 3: RMS Delay Spread for Site in Figure 2

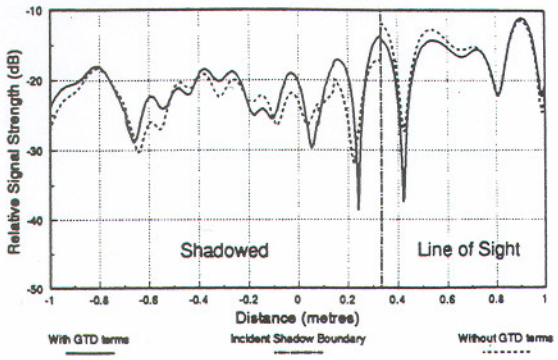

Figure 4: Signal Strength for site in Figure 2

incorporating a reflection loss. φ_k can be evaluated from the path length and knowledge of the carrier frequency with allowances being made for phase transitions resulting from reflections or diffraction. In the event of the line between transmitter and reflected receiver being intersected by more than the intersecting plane then a path is said to exist but the wave is attenuated further by passing through a blocking wall or walls.

The basic idea for the algorithm can be extended to include any number of reflections. The reflection and transmission characteristics have been evaluated as a function of arriving angle for a range of different wall materials. The algorithm has also been made more realistic by adding an antenna gain pattern to both the transmitter and receiver. Both antennas were modelled as vertically polarised half-wave dipoles.

2.2 Geometric Theory of Diffraction

The application of geometric optics provides a simple and effective method for predicting the behaviour of radio channels [7]. The method is however approximate and as such has limitations. For a non-LOS (line of sight) scenario geometric optics suffers from its exclusion of the diffracted ray paths. It was felt that in the frequency band considered here (centre frequencies 1.7 and 1.845 GHz) the effect of the diffracted rays may well be significant and thus warranted investigation.

GTD owes its origins to Keller's attempts to improve on geometric optics and has been designed as an extension to a geometric optics approach [8]. Thus the two methods can elegantly be combined to provide a single prediction tool. The formulation of diffracted paths is similar to that of reflected paths in geometric optics except that the reflection coefficient is replaced with a diffraction coefficient and alterations are made to the spatial attenuation factor. Figure 1 shows the geometry for diffraction by a straight edge. The diffracted field, for either soft (perpendicular) or hard (parallel) polarisation, resulting from a finitely conducting wedge can be calculated without singularity problems at the incidence and reflection boundaries using [9]:

$$D_s^h = \frac{-exp(-j\pi/4)}{2n\sqrt{2\pi\beta}\sin(\beta_0')}\left[\cot\left[\frac{\pi+(\varphi-\varphi')}{2n}\right]F(\beta L g^+(\varphi-\varphi'))\right.$$

$$+\cot\left[\frac{\pi-(\varphi-\varphi')}{2n}\right]F(\beta L g^-(\varphi-\varphi'))$$

$$+R_{0\perp}^{\parallel}\cot\left[\frac{\pi-(\varphi+\varphi')}{2n}\right]F(\beta L g^-(\varphi+\varphi'))$$

$$\left.+R_{n\perp}^{\parallel}\cot\left[\frac{\pi-(\varphi+\varphi')}{2n}\right]F(\beta L g^+(\varphi+\varphi'))\right] \quad (4)$$

Where the *Fresnel transition function*,

$$F(x) = 2j\sqrt{x}\exp(jx)\int_{\sqrt{x}}^{\infty}\exp(-j\tau^2)\,d\tau \quad (5)$$

and

$$L = \frac{ss'\sin^2\beta_0'}{s+s'} \quad (6)$$

$$g^{\pm}(k) = 2\cos^2\left(\frac{2\pi nN^{\pm}-k}{2}\right), \quad k=\varphi\pm\varphi' \quad (7)$$

In equation (7), $N^{\pm}$ are the integers which most closely satisfy the equations:

$$2\pi nN^{+}-(k)=\pi \quad \text{and} \quad 2\pi nN^{-}-(k)=-\pi \quad (8)$$

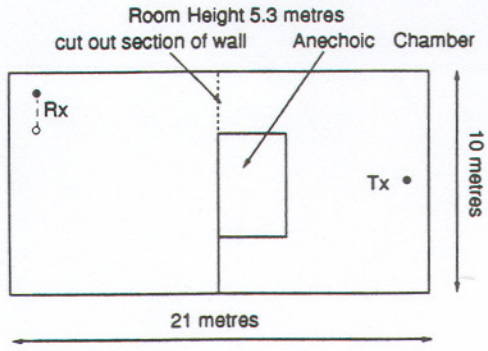

Figure 5: Indoor Site Description

$R_0^{\parallel}{}_{\perp}$ and $R_n^{\parallel}{}_{\perp}$ are the reflection coefficients for the perpendicular and parallel polarisation for the 0 face, incident angle φ', and for the n face, reflection angle $n\pi - \varphi$ (figure 2). Although the mathematical expressions for the diffraction terms look somewhat cumbersome and difficult to manipulate they can quite readily be evaluated by a computer. Calculation of the diffracted fields does however add further complexity to the algorithm and it was felt necessary to limit the computation performed. Consequently the algorithm described evaluates the first and second order diffraction terms along with all combinations of one reflection and one diffraction. For each diffracted path calculated the same path with an additional ground reflection is also evaluated.

In order to ascertain whether the diffracted rays are necessary the simple room environment of figure 2 was modelled. Figures 3 and 4 show the variation in RMS delay spread and signal strength around the incident boundary. Clearly the diffracted rays, whilst offering a little more local detail, are not having a significant impact on the overall range of predicted values for either RMS delay spread or signal strength values.

3. Channel Simulation

Results for both an indoor and an outdoor site are presented here. Figures 5 and 6 show the two sites considered. Figure 5 shows a simplified representation of the communications lab at the university. The room is divided into two main areas by a central partition and has an anechoic chamber in its centre. This site was chosen as a possible location for a radio LAN.

In figure 6, the outdoor site, the principal reflectors used within the model are shown in heavy lines, and the thinner lines with shading represent

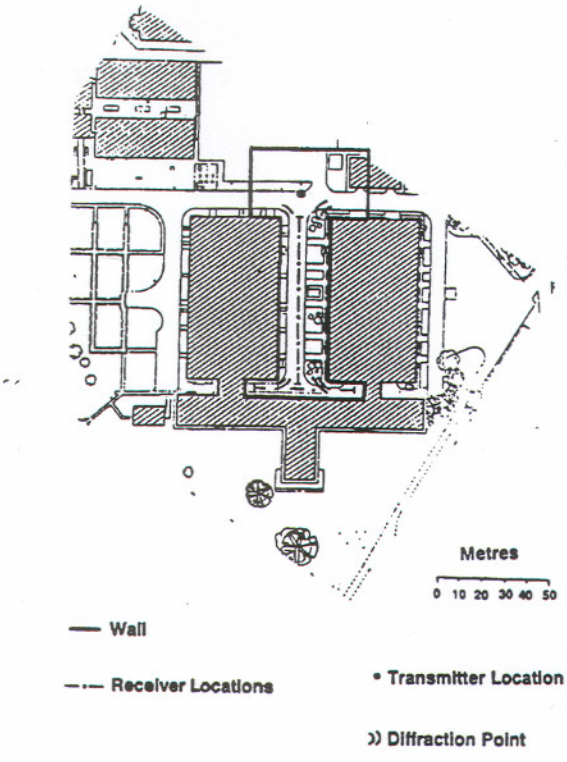

Figure 6: Outdoor Site Description

a computerised map of the area. The transmitter was placed at the end of a roadway which provided the entrance to a large 'U' shaped building surrounding three of the entrance's four sides. The area behind the transmitter is a car park which offered many potential scatterers. Measurement of both LOS and obstructed (OBS) paths were taken. The environmental description within the model is also indicated on the map. Principal reflectors, diffraction points, receiver locations are all shown. The outer cell dimensions have been bounded by reflecting planes represented by thick solid lines. This was done because it was felt that for these antenna heights (Tx = 2.5m , Rx = 1.5m) it was more likely for dissipating rays to encounter obstacles than continue in free space. This site was chosen as an example of a cordless environment serving a building entrance.

Figures 7 and 8 show the cumulative distribution function for the RMS delay spread for both measurements and modelling of the two sites. The modelled and measured results agree quite closely in each case. As expected the smaller RMS delay spread values were found indoors, with a measured range of between 7ns and 35ns with a median value of about 15ns. For the outdoor case there is

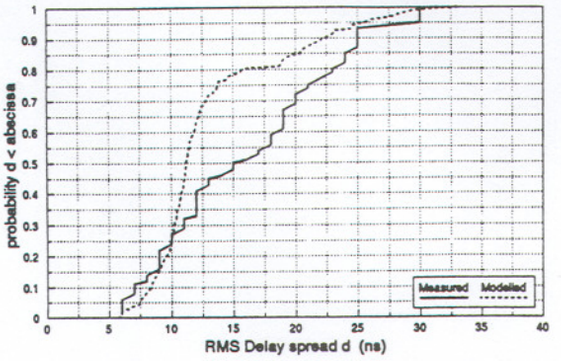

Figure 7: RMS Delay Spreads for Indoor Site

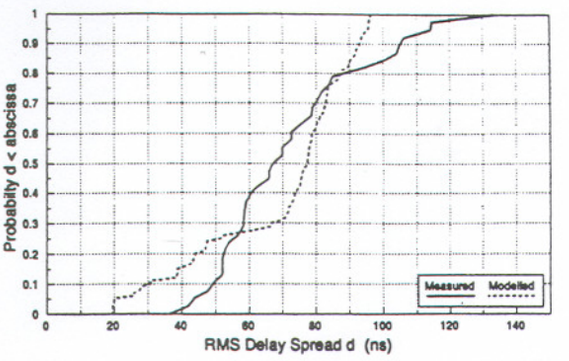

Figure 8: RMS Delay Spreads for Outdoor Site

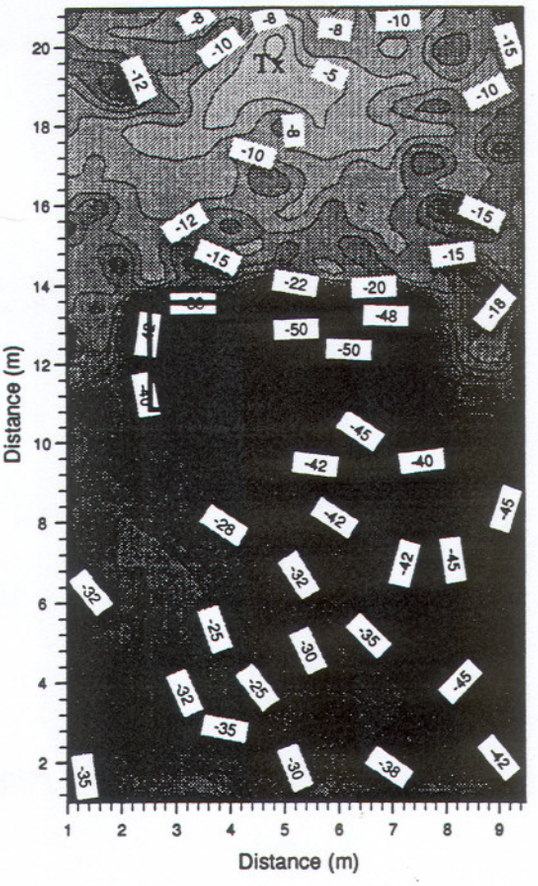

Figure 9: Indoor Signal Strength (dB)

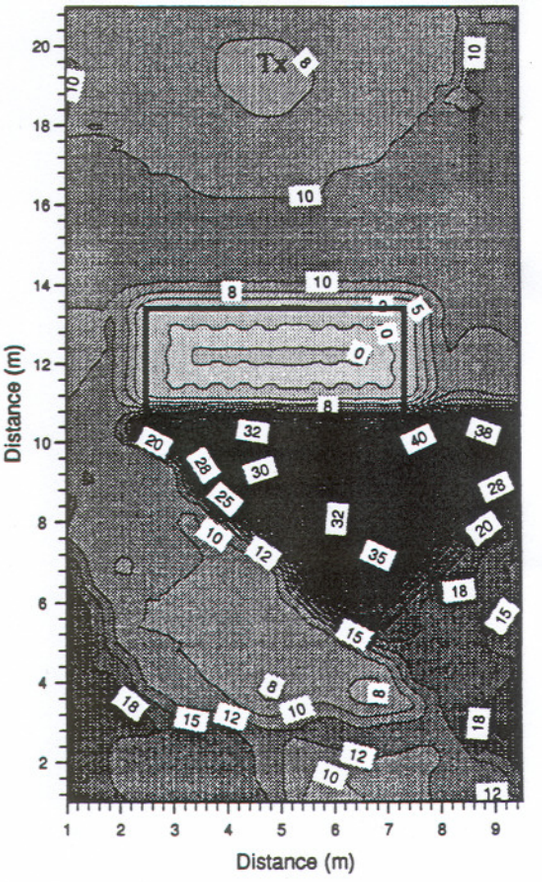

Figure 10: Indoor RMS Delay Spread (ns)

a measured range of between 40ns and 130ns with median value of 70ns. Whilst there is good agreement between modelled and measured results it is apparent that the modelled results have fewer large RMS delay spread values. This is probably because, for the outdoor case, the model confines the cell barriers at the outer perimeter and thus may fail to find the occasional distant reflected path. Also for the indoor environment the model does not calculate rays which may pass in and out of windows.

In order to consider the factors affecting both RMS delay spread and signal strength, surface contours plots have been generated for both sites, see figures 9-11 (note: values were not calculated

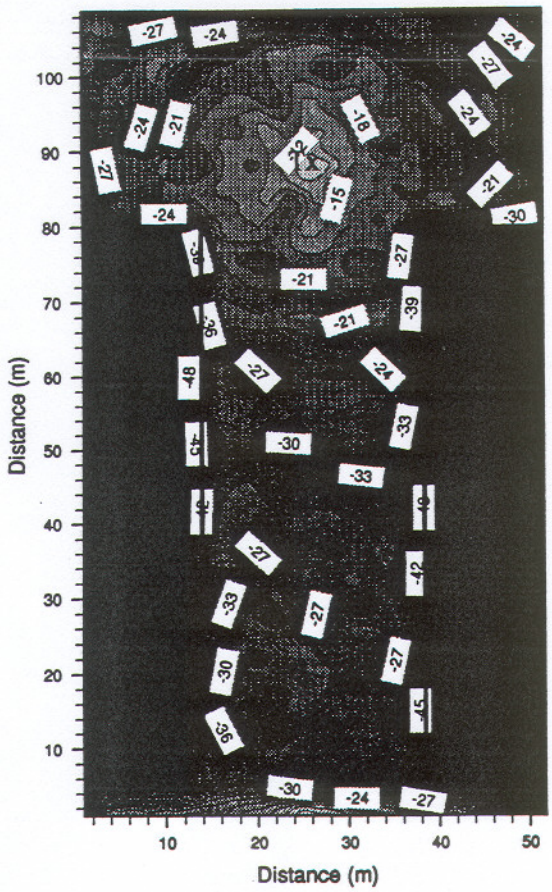

Figure 12: Outdoor Signal Strength (dB)

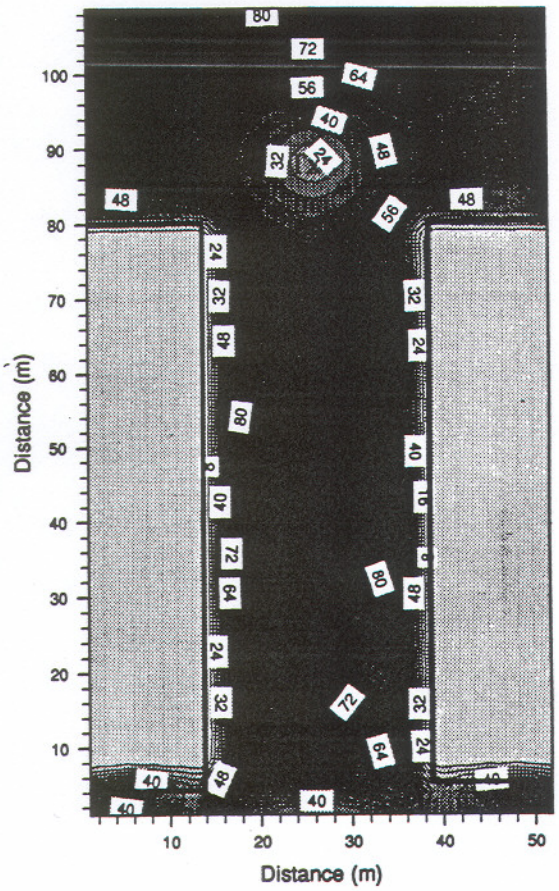

Figure 11: Outdoor RMS Delay Spread (ns)

in the anechoic chamber or inside buildings for the outdoor cell). These surface plots provide an interesting insight into the RMS delay spread and signal strength parameters. Firstly the signal strength is calculated using both amplitude and phase and as such exhibits *fast fading*. RMS delay spread however is derived from the power delay profile and therefore has no phase information and consequently exhibits no fading. The implications of this are that the signal strength data can indicate localised fades where errors may occur and, whilst a high RMS delay spread shows the dispersive nature of the channel it does not give information of where localised errors may exist. Hence due to the fast fading effects of the signal strength there is not a strong correlation between signal strength and RMS delay spread. However these results do indicate that the RMS delay spread is typically greater in shadowed regions [10]. In addition whilst cell size clearly has a bearing on the cumulative spread of RMS delay spread values there is not a strong correlation between transmitter and receiver separation and individual RMS delay spread values.

4. Modem Design

Figure 13 shows the block diagram for the transmit and receive architectures used throughout these simulations. The design was based on an IQ philosophy which allows various modulation schemes to be easily implemented in software. The transmitter simply maps the incoming data into I and Q impulse streams in accordance with the current modulation scheme. These impulses are then shaped, to bandlimit the signal, before passing them on to the RF upconverter. The demodulation process is slightly more complicated with different receivers being required for differential and differentially coherent reception. For constant envelope modulation schemes the received I and Q signals are simply mixed, as

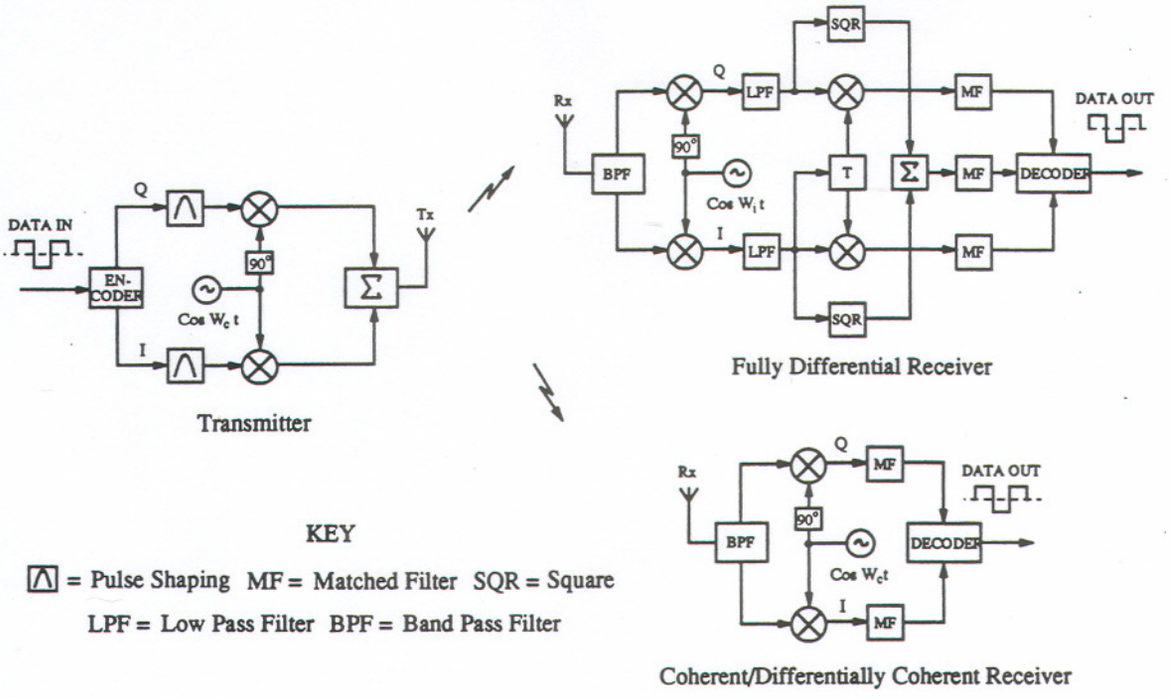

Figure 13 : Transmit and Receive Architecture

shown, to generate the required baseband data. However, for linear modulation schemes, we have included a separate circuit which extracts the signal amplitude when differential detection is required. This circuit not only maintains compatibility between the receivers but also helps to reduce the distortion introduced by the matched filters [11]. Once the amplitude and phase signals have been obtained they are mapped to the appropriate data bits in accordance with the currently selected constellation diagram. The above is a brief description of the modems operation, a more rigorous analysis has been given in [1,11].

5. Modulation

Although traditional techniques such as GMSK and QPSK have already been simulated using this software, this paper will tend to concentrate on the advantages offered using linear multi-level modulation. It is well known that 16QAM represents an optimum constellation for the reception of data in additive white Gaussian noise. However, in a fading channel it becomes difficult to track the phase variations during deep fades. This can result in the possibility of *false locking* and hence, an unacceptably high symbol error rate. These errors can be reduced by differentially encoding the transmitted data to remove its dependency on the absolute phase of the carrier. For the square QAM configuration there are a large number of possible amplitude and phase transients when differential encoding is employed across consecutive symbols. This results in a complex differential receiver which performs inadequately in noise and fading. Many alternative constellations have been proposed over the years [12,13]. In this paper we shall concentrate on the constellation shown in figure 14. This technique, referred to as 16APSK, utilises two concentric 8-PSK rings to greatly simplify the process of differential reception. A full mathematical analysis of this technique has already been evaluated and can be found in reference [1].

6. Multiple Access & Frequency Hopping

In addition to choosing a modulation scheme, a great deal of consideration must also be given to the multiple access required. If we assume that for an indoor system each user, after channel coding, transmits at up to 10 Mb/s, a TDMA system serving 15 users would then require a data rate of 150 Mb/s. Even with channel equalisation this data

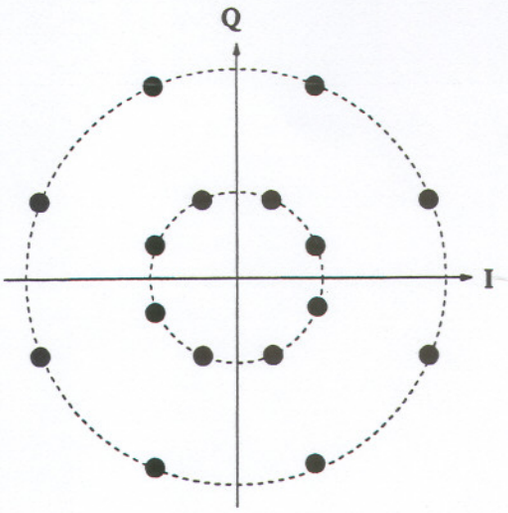

Figure 14 : 16APSK Constellation

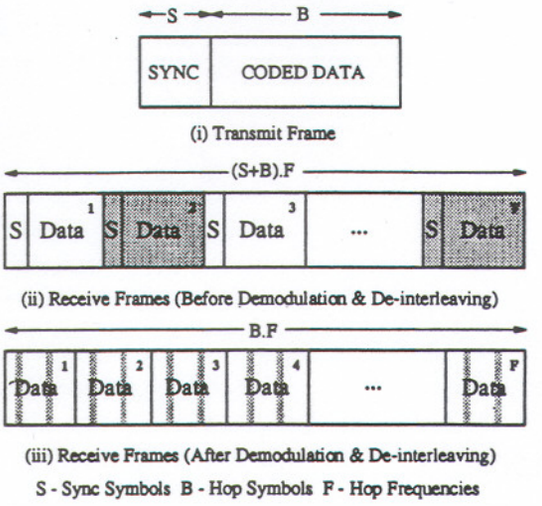

Figure 15 : Frequency Hopping & Coding

rate proves very difficult and very expensive to achieve. If each user requires a high data rate it would appear more sensible to operate using FDMA. However, there is always a chance that the frequency assigned to a user will suffer from distortion or deep signal fading, when this occurs transmission may well prove impossible. Although automatic repeat request can be applied in such situations, if the user remains on this frequency repeated transmission may not necessarily help.

It would appear impossible to guarantee the low error rates required since it is always possible for the signal to fade or suffer distortion. However, if we implement our system based on the ideas of *frequency hopping* we can, with the correct coding, operate successfully despite this corruption of the received signal [14,15]. The basic idea is illustrated in figure 15. Firstly, the data is spread out, or *interleaved*, over a number of hopping frames, each frame containing B data symbols and S synchronisation symbols. Each of these frames is then sent using a different carrier frequency, their separation being large enough to ensure uncorrelated fading. To transmit the data we can then use any differential or non-coherent modulation scheme. Coherent modulation is difficult to achieve since it requires the system to extract the carrier after each hop. Since we intend to operate in a wideband environment the symbol timing must also be acquired for each frame. If the channel is assumed stationary during frames, the synchronisation sequence may be used to obtain this information. After receiving the data it is then quite possible, due to channel distortions, for some of the frames to be received in error, this situation is denoted by the shaded regions in figure 15(ii). De-interleaving the data bits will randomise the bursts of errors thereby allowing them to be removed by the decoding process. Obviously, when too many frames arrive in error the coding scheme breaks down and is unable to correct completely the incoming data. However, by selecting the appropriate error correcting code the user can now control the error rate encountered during transmission.

To improve both the spectral efficiency and the users performance we have also assumed synchronised cyclical hopping [15]. Each user is assigned a unique pointer into a frequency look-up table, when the system is required to hop this pointer is simply incremented to obtain the next required frequency. This technique cycles through all the available frequencies in a controlled or synchronised manner thus removing any danger of data collision. This allows the overall system to fully exploit the available bandwidth.

7. System Results

The following results were all obtained using the channel models described in the earlier sections. Figure 16 shows the simulated performance of a number of different modulation schemes over a range of normalised delay spreads. The value of the normalised delay spread was calculated by simply multiplying the rms delay spread for the particular location by the simulated bit rate. The GMSK simulations were loosely based on the

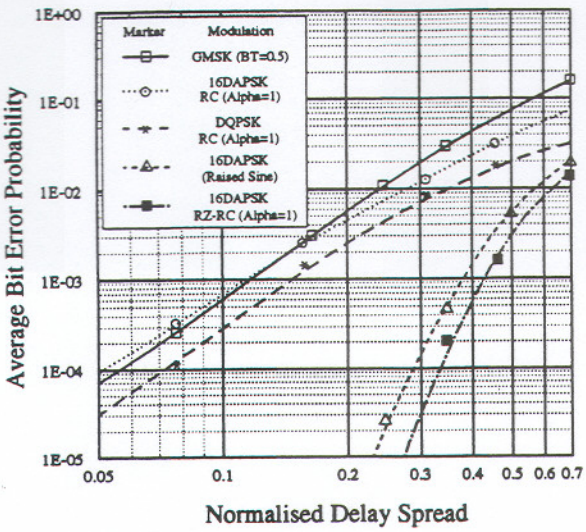

Figure 16 : Delay Spread Performance

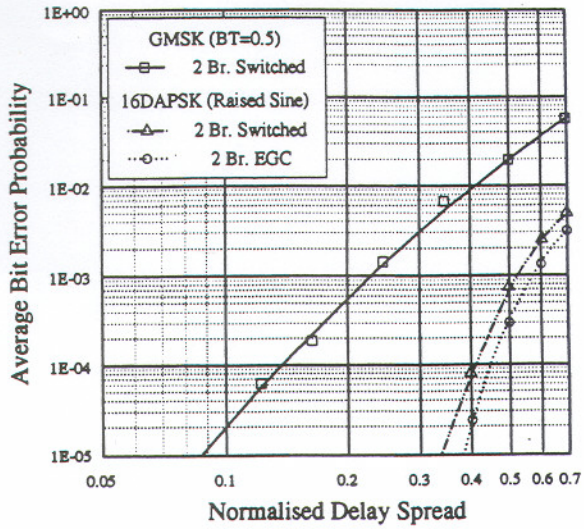

Figure 17 : Diversity Improvements

European DECT specification which, assuming a speech error threshold of 1 in 1000 bits, indicated a tolerable normalised delay spread of approximately 0.11. The performance of root raised cosine QPSK was also simulated and seen to depend on the value of the roll-off constant, α. With this value set at 1 the system performed slightly better than that for GMSK.

The 16APSK modulation scheme offered a similar order of performance, although this was achieved with a greater spectral efficiency. Using a suitable pulse shape it becomes possible to trade off this superior efficiency for improved ISI immunity. This situation has been demonstrated for two different types of anti-multipath pulse shape. The first of these uses a relatively simple raised sine time domain profile whilst the second is based on a return-to-zero root raised cosine filter (RZ-RC). This filter shapes the I and Q impulses with a root raised cosine response having a bandwidth which is twice that required by the roll-off constant. Both of these pulse shapes had the effect of lowering the bandwidth efficiency to that expected for the previous QPSK simulation. However, relative to the raised sine pulse shape, the degree of out of band energy is far less if the return-to-zero root raised cosine pulse shape is used. Based on the previous threshold, normalised delay spreads of 0.38 and 0.42 are tolerable for the raised sine and return-to-zero root raised cosine filters respectively.

Diversity is one of many techniques which can be applied to a system to reduce the impact of delay spread. Figure 17 demonstrates the diversity gains expected for two of the systems described earlier. Firstly, for the GMSK simulation, two branch switched diversity allowed the receiver to operate at normalised delay spreads up to 0.22. This figure represents a doubling of the value previously expected using a single antenna. A similar situation arose for 16APSK (using a raised sine pulse), with two branch switched diversity it now withstands a normalised delay spread of 0.51. This value is further enhanced when equal gain combining (EGC) is used. However, even with the use of diversity combining it still remains possible to encountering a signal fade. In fact, for normalised delay spreads greater than 0.7 the errors tended to occur every half a carrier wavelength. This value corresponds to the average separation distance between signal fades. For high data rates an error burst may easily last for several thousand symbol periods making forward error correction alone unable to cope. As we have already seen, applying frequency hopping to the system randomises the channel statistics and therefore allows any coding to operate successfully. Figure 18 shows the simulated effects of adding frequency hopping in a typical wideband environment. Fifteen different frequencies were simulated with a hop rate of approximately 600 hops/sec. The data was coded using a BCH(15,7) block code which was capable of correcting two bit errors in every fifteen. Without the hopping, interleaving and coding an irreducible error rate of 4 symbols in a 1000 was seen. With the hopping system enabled this irreducible error was totally removed. A significant improvement in the noise performance was also seen, although this can be mostly attributed to the sys-

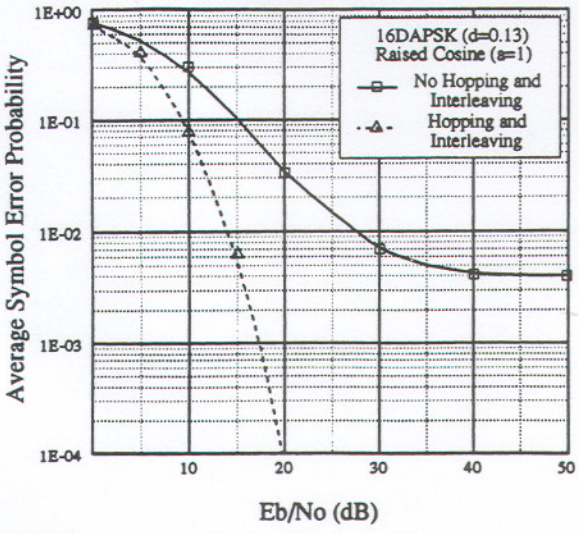

Figure 18 : Frequency Hopping - Noise Reduction

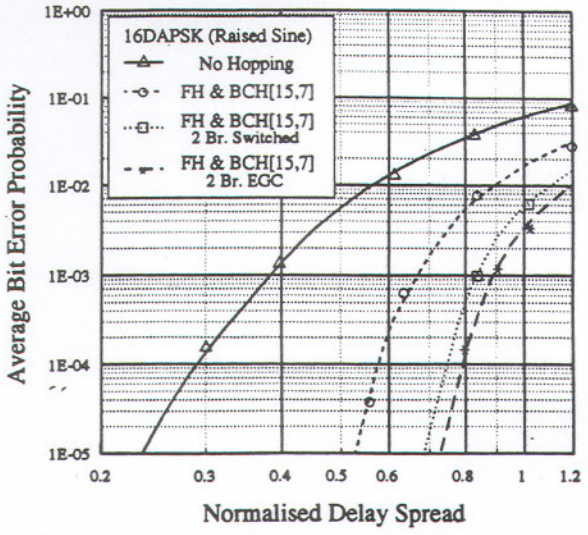

Figure 19 : Frequency Hopping in Delay Spread

tem coding. However, without the frequency hopping, the coding alone would not be able to remove the errors when the receiver moves slowly through, or remains stationary in, a signal fade.

For the hopping system, figure 19 shows the improvements in the irreducible error rate for a range of normalised delay spreads. For the previous speech threshold the unaided 16APSK receiver could tolerate a normalised delay spread of 0.38. With hopping the value is increased up to 0.65. Additional gains can also be obtained if diversity is applied to this system. Normalised delay spreads of 0.81 and 0.88 can be tolerated for switched and equal gain combining respectively.

For computer networks a more stringent error threshold needs to be defined. For the purposes of this paper we will therefore assume a data error threshold of 1 in 100000 bits. For this value, the unaided 16APSK system could tolerate a normalised delay spread of just 0.21. With frequency hopping the value increases to 0.51. Once again, diversity improves the situation with values up to 0.68 and 0.72 becoming possible for switched and equal gain combining. However, even at these low error rates additional coding or feedback error control would be needed to detect and then correct these occasional errors.

8. Conclusions

Although the irreducible error rate results have been presented in terms of normalised delay spread, providing the rms delay spread is known, these can be easily converted into their corresponding data rates. The GMSK simulation was based on DECT and therefore had a data rate of approximately 1.1Mb/s. The results indicated that for speech, up to 100ns of rms delay spread would be tolerable, 220ns if switched diversity were implemented. Considering the operating range of DECT (200m), switched diversity appears very attractive for outdoor transmissions at, or near, the cell boundaries. For example, the outdoor scenario considered in this paper showed rms delay spread up to 130ns which, without diversity, would present difficulties for a DECT based system. The QPSK results suggested a performance in delay spread similar to, or slightly better than, that for GMSK. For root raised cosine 16APSK, a similar degree of delay spread could be permitted. However, for this system, a far better spectral efficiency can be achieved.

The use of a raised sine time domain pulse reduces the sensitivity of the receiver to delay spread as well as expanding the signal bandwidth. This pulse shape now permits the 16APSK system to tolerate significantly higher values of delay spread whilst maintaining a bandwidth efficiency similar to that of both QPSK and GMSK. This improvement would allow, for the DECT environment, a maximum data rate of around 3.8Mb/s. Alternatively, keeping the data rate constant, we could now withstand rms delay spreads up to 350ns. This improved performance could then be translated into an increase in the overall cell size. Diversity was also seen to improve the performance of the 16APSK system. With equal gain combining the data rate was improved from 3.8Mb/s to 5.5Mb/s (Once again assuming an rms

delay spread of 100ns). This relatively modest improvement arises because, for larger delay spreads, the error bursts tend to lose their correlation with the received signal envelope and therefore saturate the receiving antennas. If the frequency hopping system were applied together with diversity then speech data rates as high as 8.1Mb/s and 8.8Mb/s become achievable depending on the combining techniques employed.

For computer communications such as wireless indoor networks, frequency hopping combined with an anti-multipath pulse shape has been shown to offer a suitable level of performance. The propagation models have indicated a worst case delay spread of around 35ns for the particular indoor environment considered. Using this figure we find, for the 16APSK system, that a data rate of just over 14Mb/s can be achieved with a bit error rate less than 1 in 100000. Even after the coding redundancy has been taken into account, this leaves well over 6Mb/s. If higher rates are required equal gain combining can be added to increase the gross throughput to over 20Mb/s. This would give each of the users approximately 9Mb/s. These figures compare well with the system operating without hopping, coding and diversity where data rates of around 7Mb/s were possible.

Obviously all the above figures are only applicable for the particular site considered and the modelling work has indicated that for larger environments the subsequent data rates will be reduced. However, unlike current local area networks the capacity is fixed for each user and will not reduce as the load rises. In fact, with synchronous frequency hopping, the system can run at full load whilst still avoiding the possibility of data collision. To support higher user densities it may also be possible to split each of the frequencies into several TDMA frames. This approach would then offer more flexibility in the distribution of the overall capacity.

These simulations have shown that for indoor or short range communications relatively high data rates can be achieved without resorting to channel equalisation. The choice of modulation is also important. Schemes having good spectral efficiency can always trade off this advantage to improve their ISI immunity. Hence, for a fixed bandwidth, multi-level modulation schemes will always be capable of outperforming any spectrally less efficient techniques.

Acknowledgements

The authors would like to thank SERC, BT labs, and BNR Europe Ltd. for their financial support. In addition they are grateful to BT for the provision of their channel sounding and laboratory facilities, and in particular, they wish to acknowledge the assistance of Mr P.R. Tattersall, Head of Mobile Propagation Group, for his contributive comments to the research programme. Finally the authors are indebted to their colleagues in the Centre for Communications Research, University of Bristol for the valuable advice and comments, and the provision of computing facilities. In particular we would like to thank Mr R.L. Davies for providing the indoor propagation measurements.

References

[1] A.R. Nix, R.J. Castle and J.P. McGeehan, "The application of 16APSK to mobile fading channels," *proceedings of the IEE 6th International Conference on Mobile Radio and Personal Communications*, Warwick, UK, 9-11, pp. 233-240, December 1991.

[2] F. Adachi and K. Ohno, "BER performance of QDPSK with postdetection diversity reception in mobile radio channels," *proceedings of the 41st IEEE Vehicular Technology Conference*, St Louis, USA, pp 1868-1869, May 1991.

[3] A.R. Nix and J.P. McGeehan, "Modelling and simulation of frequency selective fading using switched antenna diversity," *IEE Electronic Letters*, Vol. 26, No. 22, pp. 1868-1869, 1990.

[4] G.L. Turin, F.D. Clapp, T.L. Johnston, S.B. Fine and D. Lavry, "A statistical model for urban multipath propagation," *IEEE Trans. Vehicul. Technol.*, Vol VT-21, pp. 1-9, February 1972.

[5] H. Suzuki, "A statistical model for urban radio radio propagation," *IEEE Trans. Vehicul. Technol.*, Vol VT-40, pp. 203-210, July 1991.

[6] R. Ganesh and K. Pahlavan, "Statistical modelling and computer simulation of indoor radio channel," IEE Proc. I., Vol 138, pp. 153-161, June 1991.

[7] K.J. Gladstone and J.P. McGeehan, " A computer simulation of the effect of fading on a quasi-synchronous sideband diversity AM

movile radio scheme," *IEEE Trans. on Selected areas of Comms*, Vol. SAC-2, pp. 191-203, January 1984.

[8] J.B. Keller, "Geometrical theory of diffraction" J. Opt. Soc. Amer., Vol 52, No 2, pp. 116-130, February 1962.

[9] R.J. Leubbers, "Finite conductivity uniform GTD versus knife edge diffraction in prediction of propagation path loss" IEEE Trans. Antenn. Propag. Vol AP-32, pp. 70-76, January 1984.

[10] L.B. Lopes and M.R. Heath, "The performance of DECT in the outdoor 1.8 GHz radio channel," *proceedings of the IEE 6th International Conference on Mobile Radio and Personal Communications*, Warwick, UK, 9-11, pp. 300-307, December 1991.

[11] R.J. Castle and J.P. McGeehan, "A multi-level differential modem for narrowband fading channels," *proceedings of the 42nd IEEE Vehicular Technology Conference*, Denver, Colorado, USA, May 1992.

[12] W.J. Weber, "Differential encoding for multiple amplitude and phase shift keying systems," *IEEE Transactions on Communications, Vol. COM-26, No. 3, pp. 385-391, 1978.*

[13] W.T. Webb, L. Hanzo, R. Steele, "Bandwidth efficient QAM schemes for Rayleigh fading channels," *proceedings of the IEE 5th International Conference on Radio Receivers and Associated Systems*, Cambridge, UK, pp. 139-142, July 1990.

[14] D.J. Purle, A.R. Nix, M.A. Beach and J.P. McGeehan, "A preliminary performance evaluation of a linear frequency hopped modem," *proceedings of the 42nd IEEE Vehicular Technology Conference*, Denver, Colorado, USA, May 1992.

[15] A.A.M. Saleh, A.J. Rustako, L.J. Cimini, G.J. Owens and R.S. Roman, "An experimental TDMA indoor radio communications system using slow frequency hopping and coding," *IEEE Transactions on Communications*, Vol. 39, No. 1, pp 152-162, January 1991.